Polarization attractors in harmonic mode-locked fiber laser

Tatiana Habruseva,[1,*] Chengbo Mou,[1] Alex Rozhin,[2] and Sergey V. Sergeyev[1]

[1] *Aston Institute of Photonic Technologies, Aston University, B4 7ET, Birmingham, UK*
[2] *Aston Nanoscience Group, Aston University, B4 7ET, Birmingham, UK*
**tatiana.gabruseva@gmail.com*

Abstract: We report on a polarimetry of harmonic mode-locked erbium-doped fiber laser with carbon nanotubes saturable absorber. We find new types of vector solitons with locked, switching and precessing states of polarization. The underlying physics presents interplay between birefringence of a laser cavity created by polarization controller along with light induced anisotropy caused by polarization hole burning.

OCIS codes: (140.0140) Lasers and laser optics; (140.4050) Mode-locked lasers; (140.3510) Lasers, fiber; (160.4236) Nanomaterials.

References and links

1. S. Arahira, H. Takahashi, K. Nakamura, H. Yaegashi, and Y. Ogawa, "Polarization-, wavelength-, and filter free all-optical clock recovery in a passively mode-locked laser diode with orthogonally pumped polarization diversity configuration," IEEE J. Quantum Electron. **45**, 476–487 (2009).
2. D. Hillerkuss, R. Schmogrow, T. Schellinger, M. Jordan, M. Winter, G. Huber, T. Vallaitis, R. Bonk, P. Kleinow, F. Frey, M. Roeger, S. Koenig, A. Ludwig, A. Marculescu, J. Li, M. Hoh, M. Dreschmann, J. Meyer, S. Ben Ezra, N. Narkiss, B. Nebendahl, F. Parmigiani, P. Petropoulos, B. Resan, A. Oehler, K. Weingarten, T. Ellermeyer, J. Lutz, M. Moeller, M. Huebner, J. Becker, C. Koos, W. Freude, and J. Leuthold, "26 Tbit s(-1) 21 line-rate super-channel transmission utilizing all-optical fast Fourier transform processing," Nature Photon. **5**, 364–371 (2011).
3. J. J. McFerran, L. Nenadovic, W. C. Swann, J. B. Schlager, and N. R. Newbury, "A passively mode-locked fiber laser at 1.54 um with a fundamental repetition frequency reaching 2 GHz," Opt. Express **15**, 13155–13166 (2007).
4. T. J. Kippenberg, R. Holzwarth and S. A. Diddams, "Microresonator-based optical frequency combs," Science **332**, 555–559 (2011).
5. A. B. Grudinin and S. Gray, "Passive harmonic mode locking in soliton fiber lasers," J. Opt. Soc. Am. B **14** (1), 144–154 (1997)
6. M. S. Kang, N. Y. Joly and P. St. J. Russell, "Passive mode-locking of fiber ring laser at the 337th harmonic using gigahertz acoustic core resonances," Opt. Lett. **38**, 561–563 (2013).
7. D. Panasenko, P. Polynkin, A. Polynkin, J. V. Moloney, M. Mansuripur, and N. Peyghambarian, "Er-Yb Femtosecond ring fiber oscillator with 1.1-W average power and GHz repetition rates," IEEE Photon. Technol. Lett. **18**, 853–855 (2006).
8. C. Mou, R. Arif, A. Rozhin, and S. Turitsyn, "Passively harmonic mode locked erbium doped fiber soliton laser with carbon nanotubes based saturable absorber," Opt. Mat. Express **2**, 884–890 (2012).
9. S. Sergeyev, Ch. Mou, A. Rozhin, and S. K. Turitsyn, "Vector solitons with locked and precessing states of polarization," Opt. Express **20**, 27434–27440 (2012).
10. V. Tsatourian, S. V. Sergeyev, Ch. Mou, S. K. Turitsyn, A. Rozhin, V. Mikhailov, P. Westbrook, and B. Rabin, "Polarisation dynamics of vector soliton molecules in mode locked fibre laser," Scient. Rep. **3**, 3154, doi:10.1038/srep03154 (2013).
11. S. Sergeyev, Ch. Mou, E. Turitsyna, A. Rozhin, S. K. Turitsyn, and K. Blow, "Spiral attractor created by vector solitons," Light: Science & Applications **3**, e131, doi:10.1038/lsa.2014.12 (2014).
12. T. Udem, R. Holzwarth and T. W. Hansch, "Optical frequency metrology," Nature **416**, 233–237 (2002).

#204731 - $15.00 USD Received 15 Jan 2014; revised 3 Mar 2014; accepted 4 Mar 2014; published 13 Jun 2014

13. J. Mandon, G. Guelachvili and N. Picque, "Fourier transform spectroscopy with a laser frequency comb," Nat. Photonics **3**, 99–102 (2009).
14. G. D. VanWiggeren and R. Roy, "Communication with dynamically fluctuating states of light polarization," Phys. Rev. Lett. **88**, 097903-4 (2002).
15. L. M. Tong, V. D. Miljkovic and M. Kall, "Alignment, rotation, and spinning of single plasmonic nanoparticles and nanowires using polarization dependent optical forces," Nano. Lett. **10**, 268–273 (2010).
16. N. Kanda, T. Higuchi, H. Shimizu, K. Konishi, K. Yoshioka, and M. Kuwata-Gonokami, "The vectorial control of magnetization by light," Nature Commun. **2**, 1–5 (2011).
17. S. M. J. Kelly, "Characteristic sideband instability of periodically amplified average soliton," Electron. Lett. **28**, 806–807 (1992).
18. F. Li, E. Ding, J. N. Kutz, and P. K. A. Wai, "Dual transmission filters for enhanced energy in mode-locked fiber lasers," / Opt. Express **19**, 23408–23419 (2011).
19. L. Yun, X. Liu and D. Mao, "Observation of dual-wavelength dissipative solitons in a figure-eight erbium-doped fiber laser," Opt. Express **20** (19), 20992–20997 (2012).
20. H. Zhang, D. Y. Tang, X. Wu, and L. M. Zhao, "Multi-wavelength dissipative soliton operation of an erbium-doped fiber laser," Opt. Express **17**, 12692–12697 (2009).
21. N. Akhmediev and J. M. Soto-Crespo, "Dynamics of soliton-like pulse-propagation in birefringent optical fibers," Phys. Rev. E **49**, 5742–5754 (1994).
22. L. M. Zhao, D. Y. Tang, T. H. Cheng, C. Lu, H. Y. Tam, X. Q. Fu, and S. C. Wen, "Passive harmonic mode locking of soliton bunches in a fiber ring laser," Optical and Quantum Electronics **40** (13), 1053–1064 (2009).

1. Introduction

High repetition rate mode-locked fiber lasers (MLFLs) are of interest for telecommunication applications in the context of optical time-domain multiplexing, all-optical clock recovery [1], orthogonal frequency division multiplexing [2]. Typically, MLFLs operate at repetition rate in the order of MHz due to the relatively long laser cavity. Higher repetition rates can be achieved in passive MLFLs by shortening cavity lengths below 20 cm [3], introducing comb filters [4], and increase of the pump power resulting in soliton breakup and harmonic mode-locking [5]. When compared to active mode-locking techniques, passive mode-locking has reduced complexity and a potential to obtain shorter optical pulses at high repetition rates [6–8].

Harmonic MLFLs based on carbon nanotubes (CNTs) demonstrated sub-picosecond pulses at high repetition rates [8]. The polarization insensitivity of CNTs based saturable absorber extends possibilities of studying polarization attractors in MLFLs [9–11]. Recently, polarization dynamics in MLFLs has been exploited to reveal impact on the pulse train stability for fundamental, multi-pulse and bound states soliton operation [9–11]. The stability of pulse trains in MLFLs is an important issue for increased resolution in metrology [12], high precision spectroscopy [13] and suppressed phase noise in high speed fibre optic communications [2].

In this paper we demonstrate experimentally, for the first time to our knowledge, polarization dynamics of harmonic mode-locked operation in erbium doped fiber laser with CNTs based saturable absorber. We achieve up to 11th harmonic mode-locking with over 50 dB sidebands suppression ratio. We reveal novel vector soliton types for multi-pulse and harmonic mode-locked operation with locked, switched and precessing SOPs. The results can have potential applications for increased capacity in coherent communications using various polarization-based modulation schemes, such as polarization division multiplexing, polarization switching, and modified coded hybrid subcarrier-amplitude-phase-polarization multiplexing [1, 2]. High flexibility in generation of dynamic polarization states can be also of interest in secure communications [14], atoms and nanoparticles trapping [15], and control of magnetization [16].

2. Experiment

The fiber laser configuration is shown in Fig. 1. The ring cavity with the total length of 7.8 m consisted of a 40 cm long highly erbium-doped gain fiber (LIEKKI $110-4$, group velocity dispersion parameter $\beta_{2,EDF} = +12.6 ps^2/km$)), a single mode fiber with anomalous dispersion

#204731 - $15.00 USD Received 15 Jan 2014; revised 3 Mar 2014; accepted 4 Mar 2014; published 13 Jun 2014

(SMF-28, $\beta_{2,SMF} = -22.8 ps^2/km$), a 99/1 tap, a fiber isolator, a polarization controller (PC), an output coupler, a saturable absorber and a wavelength division multiplexing (WDM) coupler. The gain fiber was pumped at 976 nm by a a fiber grating stabilized laser diode via a 980/1550 nm WDM coupler and a PC. To avoid connectors and CNTs damage the maximum current applied to the pump laser was 300 mA, which provided 170 mW of optical power. We used a single-wall CNTs polymer film embedded between standard FC/APC fiber connectors as a saturable absorber. An index matching gel was applied to minimize the transmission losses. CNTs films preparation and characterization was as described in [8]. 10% of the laser output was coupled out of the cavity and characterized by optical and electronic spectrum analyzers (ANDO AQ6317B and HP8562), an inline polarimeter (Thorlabs, IPM5300) and a fast oscilloscope (Tektronix DPO7254). The dynamics of SOP was measured using the polarimeter, which

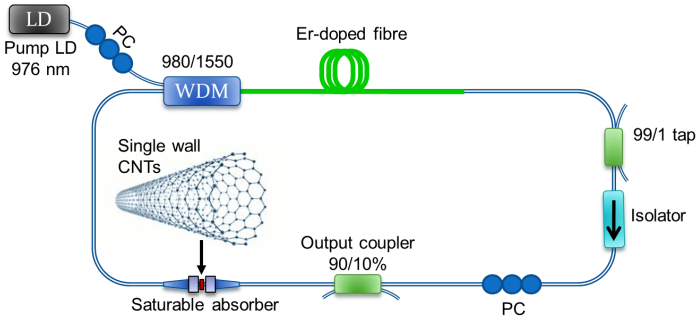

Fig. 1. Configuration of Erbium doped fiber laser with single wall carbon nanotubes (CNTs) saturable absorber. LD: laser diode, PC: polarization controller, WDM: wavelength division multiplexing coupler.

produced 1024 samples with 1 μs resolution (25 round-trip times) giving the normalized Stokes parameters s_1, s_2, s_3, a total output power and a degree of polarization (DOP). The Stokes parameters are related to the powers of two linearly cross-polarized SOPs, $|u|^2$ and $|v|^2$, and phase difference between them, $\Delta\phi$, as follows:

$$S_0 = |u|^2 + |v|^2; S_1 = |u|^2 - |v|^2; S_2 = 2|u||v|cos(\Delta\phi); S_3 = 2|u||v|sin(\Delta\phi). \quad (1)$$

The normalized Stokes parameters s_1, s_2, s_3, and a degree of polarization (DOP) are defined as:

$$s_{1,2,3} = \frac{S_{1,2,3}}{\sqrt{S_1^2 + S_2^2 + S_3^2}}; DOP = \frac{\sqrt{S_1^2 + S_2^2 + S_3^2}}{S_0}. \quad (2)$$

The evolution of normalized Stokes parameters over time produces a track on the Poincaré sphere, which is commonly used to visualize polarization dynamics. In experiments, the pump power was varied and various polarization attractors were obtained by tuning both the intracavity and pump laser PCs.

3. Polarization attractors

The CW lasing started at $\sim$ 35 mW pump power with the fundamental mode-locking starting at $\sim$ 45 mW pump power. The cavity round-trip time was $\sim$ 39 ns, which corresponded to 25.5 MHz pulse repetition rate in fundamental mode-locked regime. The total anomalous cavity

#204731 - $15.00 USD Received 15 Jan 2014; revised 3 Mar 2014; accepted 4 Mar 2014; published 13 Jun 2014

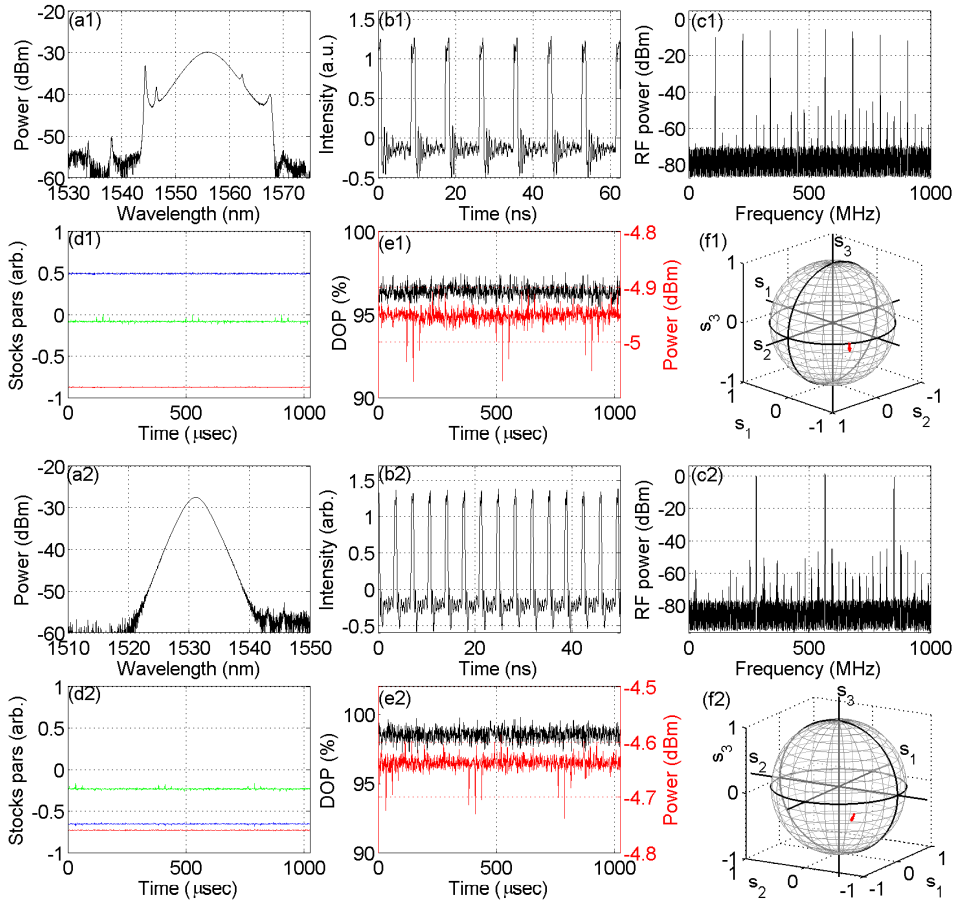

Fig. 2. Polarization-locked vector solitons at (a1-f1) 4th harmonic (pump power 133 mW), and (a2-f2) 10th harmonics (pump power 162 mW). (a) Optical spectra, (b) pulse trains, (c) RF spectra, (d) normalized Stocks parameters, s_1 (red), s_2 (blue), s_3 (green), (e) degrees of polarization (black) and output powers (red), (f) Poincaré spheres.

dispersion resulted in soliton-shaped output pulses with typical Kelly sidebands in the optical spectrum [17]. Pump power increase resulted in the multiple-pulsing and harmonic mode-locked laser operation, with a higher pump power leading to a larger number of solitons and higher harmonics. This multi-pulsing arises due to limited cavity bandwidth constraints [5, 18]. Low noise harmonic mode-locking was achieved with over 50 dB sidebands suppression ratio up to 11th harmonic with 310 MHz pulse repetition rate. The sidebands increased for 13th and 14th harmonics.

Tuning of the intra-cavity PC resulted in a large diversity of the laser operation regimes, including harmonic mode-locking, bound states and multi-pulsing. By varying the intra-cavity PC we could achieve vector solitons with different polarization dynamics, such as polarization-locked vector solitons, solitons with precessing, switching and chaotic SOP [9]. Polarization-locked vector solitons could be obtained for different harmonics and fundamental mode-locking. Figure 2 shows examples of polarization-locked vector solitons at 4th (Figs. 2(a1)-2(f1)) and 10th (Figs. 2(a2)-2(f2)) harmonics, respectively. Constant Stokes parameters and a high DOP indicates stable output polarization over averaging time. The regimes stability was

#204731 - $15.00 USD Received 15 Jan 2014; revised 3 Mar 2014; accepted 4 Mar 2014; published 13 Jun 2014

tested over several hours time.

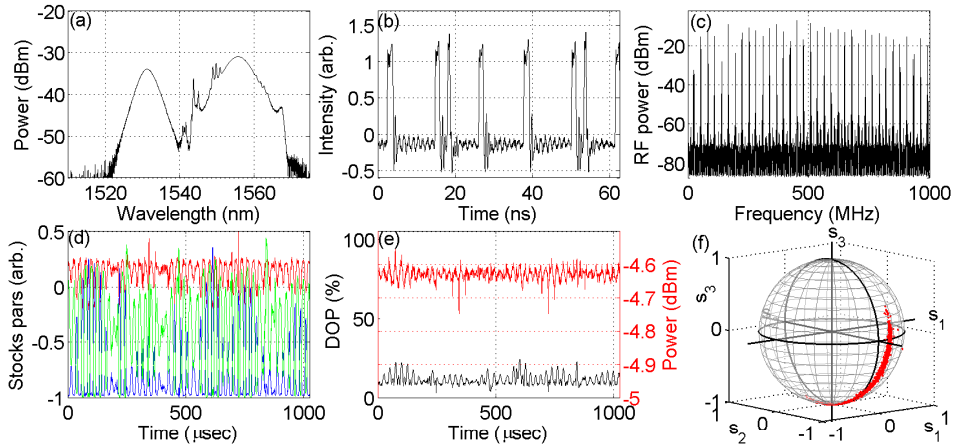

Fig. 3. Combination of vector solitons at the fundamental and 3rd harmonic with slowly evolving polarization. (a) optical spectrum, (b) pulse train, (c) RF spectrum, (d) normalized Stocks parameters, s_1 (red), s_2 (blue), s_3 (green), (e) degree of polarization (black) and output power (red), (d) Poincaré sphere. Pump power 147 mW.

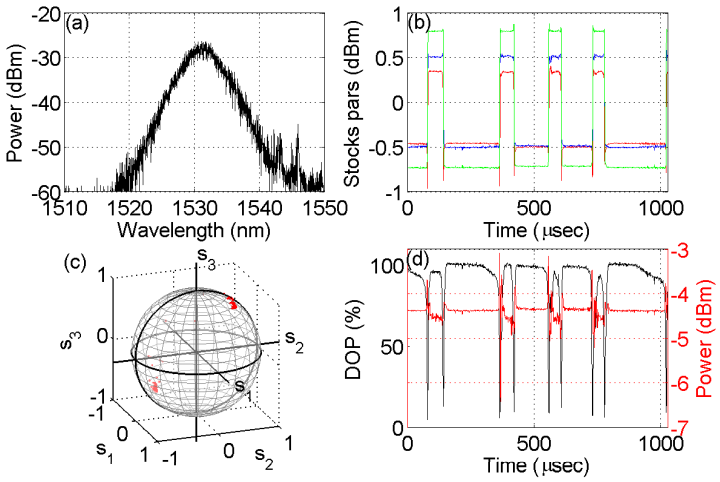

Fig. 4. Solitons group with switching polarization. (a) optical spectrum, (b) normalized Stocks parameters, (c) Poincaré sphere, (d) degree of polarization (black) and output power (red). Pump power 170 mW.

Pump power increase to 147 mW (250 mA) lead to a dual-wavelength laser operation with optical spectra centered at 1555.5 nm and 1531 nm, as shown in Fig. 3(a). This complex optical spectrum shape results due to combination of solitons at the fundamental and 3rd harmonic. Figure 3(b) shows a snapshot of the pulse train measured with the scope. The pulses at the fundamental and 3rd harmonic have different group velocities and were drifting on the scope from each other. Similar results obtained for figure-of-eight and SESAM-based fibre lasers suggest that this dual-wavelength behavior can be attributed to the birefringence-induced filtering effect [19, 20]. The laser output demonstrated a slowly evolving SOP with a sector-type attractor

#204731 - $15.00 USD Received 15 Jan 2014; revised 3 Mar 2014; accepted 4 Mar 2014; published 13 Jun 2014

on the Poincaré sphere. This attractor type can arise as a result of fast SOP rotation and a low-pass filter implemented by the polarimeter's photodetector with a 1 MHz bandwidth [11]. The combination of solitons at the fundamental and 4th harmonic was also observed.

The further increase of the pump power to 170 mW resulted in the shift of the lasing spectrum to 1531 nm. Figure 4 demonstrates unstable operation with polarization switching between two cross-polarized SOPs (c). Blurred contour of optical spectrum in Fig. 4(a) indicates that output power is fluctuating during the time of polarization switching, as shown in Fig. 4(d). Optical spectrum summarizes different polarization states and hence represents unstable shape. Figures 4(b) and 4(d) indicate slow dynamics of Stokes parameters, DOP and output power averaged over 25 round trips. The high DOP between the polarization switching points in Fig. 4(d) reveals identical polarization of the solitons bunch, and the quasi-stable regions between polarization switches in Fig. 4(b) indicate the constant SOP of the solitons over $60-240\mu$sec. Two orthogonal SOPs correspond to the eigenvalues of the stable vector solitons solutions [21]. The periodic character of the switches and unequal residence time at the orthogonal SOPs suggest the presence of polarization instabilities caused by polarization hole burning and anisotropy of pumping [11]. If the pump SOP deviates from the circular one, averaged anisotropy is present resulting in preference for one of the cross-polarized SOPs. From [11], the absorption cross section of an elliptically polarized pump with an ellipticity δ is given by:

$$\sigma_{a,p} = \sigma_a^{(p)}(cos^2(\theta)+\delta^2 sin^2(\theta))/(1+\delta^2), \tag{3}$$

where $\sigma_{a,p}$ is the absorption cross section of the elliptically polarized light, $\sigma_a^{(p)}$ is the cross section of the circular polarized light with $\delta = 1$, θ is the angle between dipole moment of absorption at the pump wavelength and unit vector along the pump field. Thus, the pump light creates an orientational distribution of the population inversion $n(\theta)$, i.e. anisotropy, if $\delta \neq 1$. The lasing field $E = u\mathbf{e_x} + v\mathbf{e_y}$ burns a hole in this distribution with the depth [11]:

$$h(\theta) \sim |u|^2 cos^2(\theta) + |v|^2 sin^2(\theta) + 2|u||v|cos(\Delta\phi)cos(\theta)sin(\theta)). \tag{4}$$

The depth of a polarization hole depends on the phase difference $\Delta\phi$ and the powers of cross polarized components of the lasing field, $|u|^2$ and $|v|^2$.

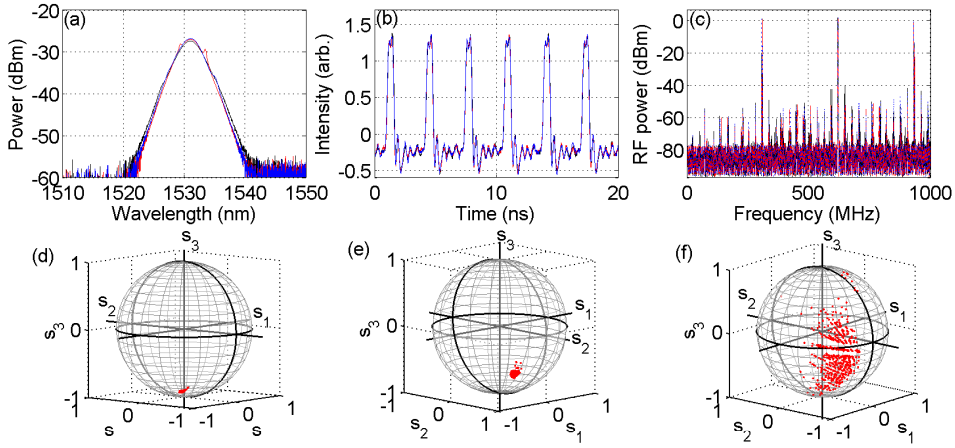

Fig. 5. Vector solitons at 11th harmonic with (d) stable, (e) precessing in microsecond scale, and (f) chaotic polarization. (a) Optical spectra, (b) pulse trains, (c) RF spectra for stable (black), precessing (red), and chaotic (blue) polarization, (d-e) Poincaré spheres.

#204731 - $15.00 USD Received 15 Jan 2014; revised 3 Mar 2014; accepted 4 Mar 2014; published 13 Jun 2014

Varying intra-cavity PC yielded vector solitons with different polarization attractors. Figure 5 shows vector solitons at 11th harmonic with (d) stable polarization, (e) slow polarization precession in microsecond scale, and (f) chaotic polarization. Corresponding optical spectra, pulse trains and RF spectra are overlapped in Figs. 5(a)-5(c) for all three cases. Remarkably, optical (a), RF spectra (c) and pulse trains (b) were nearly identical for all three regimes, and only polarization attractors could reveal the differences. Only polarimetry along with polarization control and characterization of pulse traces, optical and electronic spectra gives us opportunity to stabilize SOP of 11th harmonic of a single pulse rather than bound state or multi-pulsing operation [10, 22], which is important for many applications involving polarization-based modulation schemes [1, 2].

4. Conclusion

For the first time we have measured polarization attractors of a harmonic mode-locked fiber laser. Polarization-locked vector solitons were obtained at all harmonics studied and fundamental mode-locking. The pump power increase to 147 mW yielded the dual-wavelength laser operation with central wavelengths at 1555.5 and 1531 nm. This complex optical spectrum corresponded to a co-existence of vector solitons traveling at the fundamental and 3rd harmonics and can be attributed to the birefringence-induced filtering effect [19, 20].

The laser optical spectrum shifted to 1531 nm at the further pump power increase to 170 mW. The novel regime with polarization switching between two orthogonal SOP was shown for the grouped solitons. The quasi stable periodic dynamics of the Stokes parameters indicates the influence of the light induced anisotropy caused by polarization hole burning. Finally, vector solitons with various polarization attractors were shown at the 11th harmonic, which have a potential application in high capacity fiber optic communications, in the context of using multiple polarizations rather than polarization division multiplexing schemes [1], and can be used in secure communications [14].

Acknowledgments

This work was funded by the Marie Curie Action FP7-PEOPLE-2011-IEF, HARMOFIRE project, Grant No 299288, by the EPSRC (project UNLOC, EP/J017582/1), European Research Council (ULTRALASER) and FP7-PEOPLE-2012 IAPP (project GRIFFON, No 324391).

#204731 - $15.00 USD Received 15 Jan 2014; revised 3 Mar 2014; accepted 4 Mar 2014; published 13 Jun 2014